



Fabricating durable and stable superhydrophobic coatings by the atmospheric pressure plasma polymerisation of hexamethyldisiloxane

Sultan S. Ussenkhan^{a,b}, Baglan A. Kyrykbay^{a,b}, Yerassyl Yerlanuly^{a,b,c,*}, Askar T. Zhunisbekov^b, Maratbek T. Gabdullin^c, Tlekkabul S. Ramazanov^b, Sagi A. Orazbayev^{a,b,***}, Almasbek U. Utegenov^{a,b,c,**}

^a Institute of Applied Science and Information Technologies, 280 Bayzakov str., 050038, Almaty, Kazakhstan

^b Al-Farabi Kazakh National University, 71/23 Al-Farabi Ave., 050040, Almaty, Kazakhstan

^c Kazakh-British Technical University, 59 Tole Bi Str., 050000, Almaty, Kazakhstan

ARTICLE INFO

Keywords:

Atmospheric discharge plasmas
Contact angles
Hexamethyldisiloxane
Plasma polymerisation
Superhydrophobic surface

ABSTRACT

The paper was devoted to the results of the study of methods to obtain superhydrophobic film based on the plasma polymerisation of hexamethyldisiloxane (HMDSO) inside the plasma jet at atmospheric pressure. The 3D printing technology was intended for film deposition, which has the advantage of producing superhydrophobic surfaces over a wide range of scales. The effect of synthesis parameters on the hydrophobic properties of the film has been studied. The obtained superhydrophobic films demonstrated stability and resistance in chemical solutions, at high temperatures, under the influence of UV-irradiation and in various weather conditions. The results can be used in various fields, including automotive, construction, electronics, medicine and others, where surface protection against moisture, contamination and corrosion is required.

1. Introduction

The superhydrophobic surface has an extremely high water-repellency and is designed to prevent water from sticking, collecting and rolling off like mercury drops. Over the last decade, superhydrophobic coatings with a contact angle greater than 150° have been produced with the aim of achieving a 'lotus effect' on the surface of various materials. These coatings are of great interest due to their attractive properties such as water resistance [1], self-cleaning [2], corrosion protection [3], anti-fogging [4], anti-icing [5], biofouling protection [6], anti-friction properties [7] etc. Due to their unique properties, hydrophobic films have a great potential for practical applications and can be used in power engineering, construction, medicine, marine industry, aviation, textiles, etc. [8–11], for self-cleaning [11], flow resistance reduction [12], anti-icing [5,13], corrosion protection [14], oil and water separation [15,16].

Surface hydrophobicity depends on two factors: the surface topography of the material (micro-nanotextured roughness) and its chemical composition (low surface energy) [15]. The superhydrophobic effect arises from micro- and nanoscale features that create a

* Corresponding author. Institute of Applied Science and Information Technologies, 050038 Almaty, Kazakhstan.

** Corresponding author. Al-Farabi Kazakh National University, 050040 Almaty, Kazakhstan.

*** Corresponding author. Institute of Applied Science and Information Technologies, 050038 Almaty, Kazakhstan.

E-mail addresses: yerlanuly@physics.kz (Y. Yerlanuly), sagi.orazbayev@gmail.com (S.A. Orazbayev), almasbek@physics.kz (A.U. Utegenov).

Abbreviations

HMDSO	hexamethyldisiloxane
SEM	scanning electron microscopy
CVD	chemical vapour deposition
DI	deionized water

rough textured surface and minimize the contact area between water droplets and the film, reducing the adhesive force between them [17,18]. As a result, water droplets are repelled from the surface and easily slip off, removing with them any dirt, dust or other contaminants that may be attended.

At this stage of development, there are many methods of producing hydrophobic and superhydrophobic surfaces based on obtaining a rough topography. These methods can be classified under the conception of nanofabrication by 'top-down' and 'bottom-up' approaches [19]. Top-down methods include lithography and plasma treatment [20,21]. Bottom-up methods characterise the colloidal assembly, layer-by-layer (LbL) and chemical vapour deposition (CVD), plasma polymerisation [22–24].

Among the mentioned above methods, chemical methods and atmospheric pressure plasma polymerisation are economically feasible and suitable for large scale production. Undoubtedly, chemical methods can produce superhydrophobic coatings with good transparency and mechanical strength. However, most of these methods rely on the use of toxic solvents and liquid chemical compounds, mainly from organosilanes and fluorinated chemicals [25] which vapours are harmful to the human body and the environment. Additionally, these methods require multilayer deposition [26] to obtain a hydrophobic film, and immersion [27] or centrifugation [28] methods are commonly used to uniformly distribute the film, which also complicates the process of depositing the film into existing systems and increases the time to obtain a coating. Therefore, the study and development of a one-step coating method that is scalable, inexpensive, simple and environmentally friendly is a very urgent task. One of the most promising and environmentally friendly methods is atmospheric plasma polymerisation [29,30]. The advantage of using atmospheric pressure plasma compared with other existing plasma technologies for producing superhydrophobic surfaces [31,32] is rest on irrelevant for expensive vacuum facilities or the use of chemical compounds that may be harmful to human health, making it an economical and environmentally friendly technology. In addition, the plasma method allows for extensive control of the synthesis parameters [33], thereby influencing the properties of the resulting material. The production of hydrophobic surfaces using atmospheric pressure plasma is a relevant and prospective area of research.

Despite the many potential applications of a superhydrophobic surface, there are still open issues that need to be solved. One of these is the durability, stability and resistance of hydrophobic surfaces to extreme conditions [14,34–36], as they can be damaged by critical temperatures, mechanical, chemical and UV exposure. Moreover, although many of the existing technologies for producing a superhydrophobic surface are time consuming and financially demanding [37–39], finding alternative methods and improving

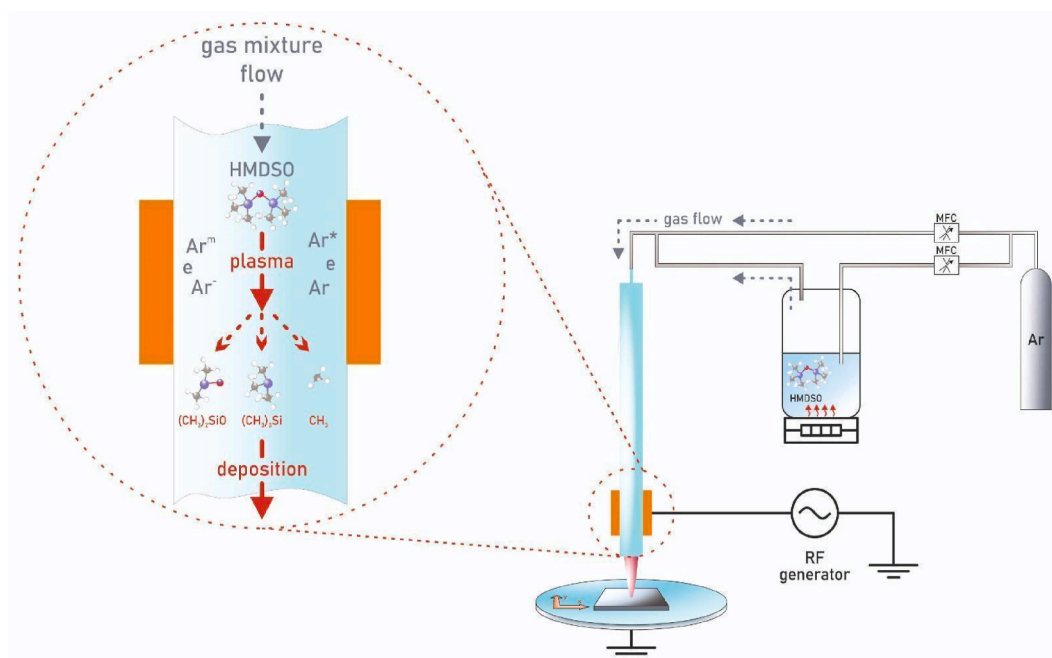


Fig. 1. Schematic of an experimental setup for the deposition of a superhydrophobic film by plasma polymerisation at atmospheric pressure.

existing methods that are more compatible with large-scale industrial production is now becoming a hot topic [40].

This paper presents a method to produce a superhydrophobic surface based on HMDSO plasma polymerisation at atmospheric pressure with RF discharge using 3D printing technology for large scale surface treatment. The effect of plasma parameters, number of cycles, and precursor flow on the formation of the superhydrophobic surface was investigated. Characterisation of the obtained results was carried out by SEM, X-ray photoelectron spectroscopy (XPS) (to determine the elemental composition and having bonds on the surface of the obtained film). The optical emission spectrum of the OES plasma was investigated to determine the mechanism of hydrophobic coating formation. In addition, studies were carried out to determine the resistance, stability and durability of the resulting superhydrophobic coatings at critical temperatures and under extreme conditions. The ability of the resulting superhydrophobic films to act as self-cleaning surfaces has been demonstrated. These studies will allow the use of superhydrophobic coatings to be extended to various applications where effective protection of surfaces against moisture, dirt and corrosion is required.

2. Experimental section

2.1. Materials

Hexamethyldisiloxane (HMDSO $\geq 98\%$), Acetone (99.5%), 2-propanol (IPA, 99.9%), were both purchased from Sigma-Aldrich Company and used as received without any further purification steps. Solvent 646 was purchased from Com Trade LLP. Ethyl alcohol (90%) was purchased from PHARMACIA LLP.

2.2. Production of hydrophobic films

Prior to treatment, the substrates were cleaned in the following sequence: Hellmanex™ III detergent solution in DI water, DI water,

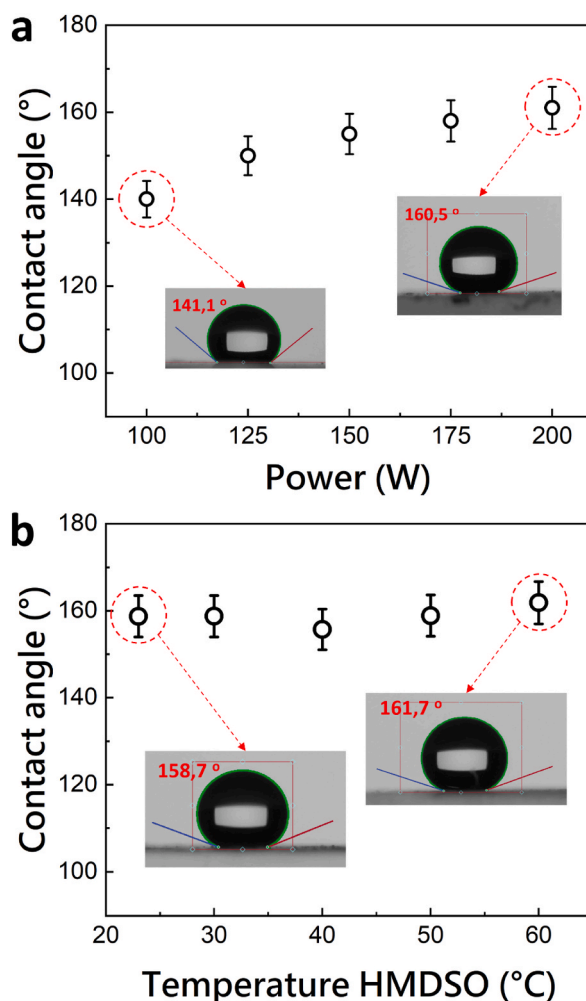


Fig. 2. Graphs of contact angle versus discharge power (a) and HMDSO temperature (b).

acetone and 2-propanol. Each cleaning step was performed in an ultrasonic bath for 10 min. The thin film was deposited by plasma polymerisation at atmospheric pressure.

Fig. 1 shows a schematic of the experimental setup for generating a plasma jet at atmospheric pressure (the setup itself is shown in Fig. S1, the workflow for applying the superhydrophobic film is shown in Fig. S2 and in the video S1 in the supporting information). The setup consisted of a quartz tube with outer and inner diameters 6 mm and 3 mm, respectively, electrodes and a working gas supply system. A copper strip wrapped around the quartz tube was used as the high voltage electrode and a copper plate on the bottom was used as the grounded electrode. Such a configuration of electrodes (with parallel direction of gas flow and electric field) ensured rapid formation of the film on the sample. A quartz glass plate was used to create a dielectric barrier above the ground electrode. The Seren R301 power supply generated sinusoidal signals at a frequency of 13.56 MHz. The working gas was argon and the precursor was HMDSO. The selection of the HMDSO as a precursor is due to its non-toxicity and relative safety [41], which makes them preferable to other organosilanes that are commonly used for the preparation of organosilicon thin films. Moreover, HMDSO has the complementary advantage that it offers a higher vapour pressure at room temperature (48 Torr) [42,43], which facilitates its application in vapour deposition processes. A bubbler was used to produce HMDSO vapour as it is a liquid at room temperature. The main argon flow and HMDSO vapour concentration were controlled by the mass flow controllers. Glass and silicon samples of 2×2 cm were used as substrates. A CNC3018 3D plotter was used to deposit the film and control the distance from the tube nozzle to the substrate. The rate of sample movement is 10 mm/s. Processing time for a 1 square inch glass sample is 70 s.

2.3. Characterisation methods

All samples were tested under normal environmental conditions and water was used to measure the contact angle. A scanning electron microscope (Quanta 3D 200i, SEM FEI company) was used to analyse the surface morphology (roughness) and chemical composition of the obtained samples. X-Ray Photoelectron spectroscopy with an Al K α monochromatic X-ray source at 1486.6 eV (XPS, NEXSA, Thermo Scientific) was used to study the chemical composition of the surface of the obtained films. The optical properties of

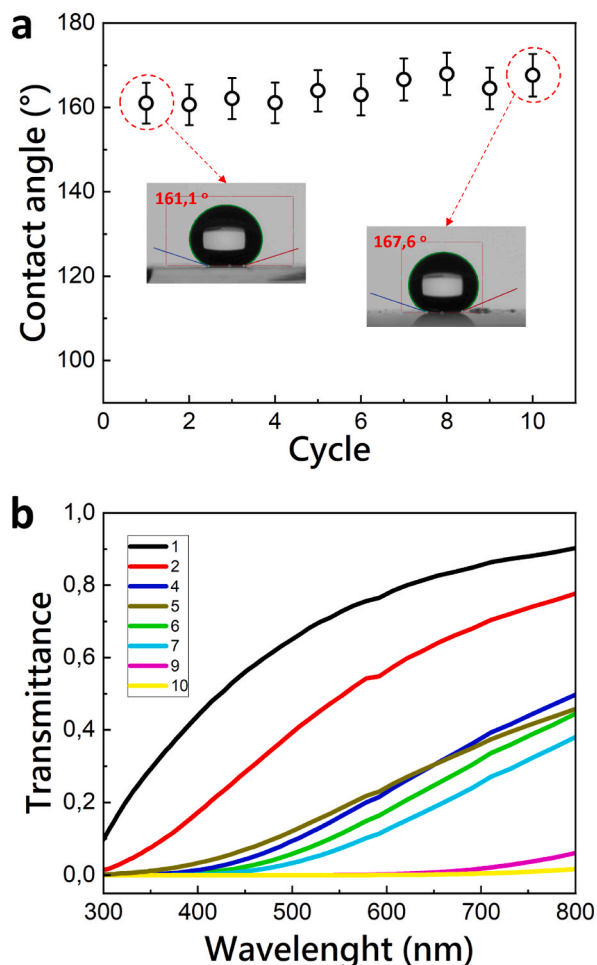


Fig. 3. Graphs of contact angle versus number of cycles (a) and transmittance (b).

thin films were analysed using spectroscopic ellipsometry (Horiba-Universal-Plus). An Optosky ATP2000 spectrometer was used to study the optical spectrum of the plasma. The contact angle was measured using a goniometer (Contact Angle Goniometer, Ossila). The AREC Heating magnetic Stritter was used as the heater. A 100 W PPBL-ZG N29 lamp was used for the UV testing.

3. Results and discussion

In order to determine the optimum plasma parameters for the formation of a superhydrophobic surface, experiments were first carried out to investigate the effect of discharge power on the contact angle of the film. The Ar and Ar + HMDSO gas flow rates were set

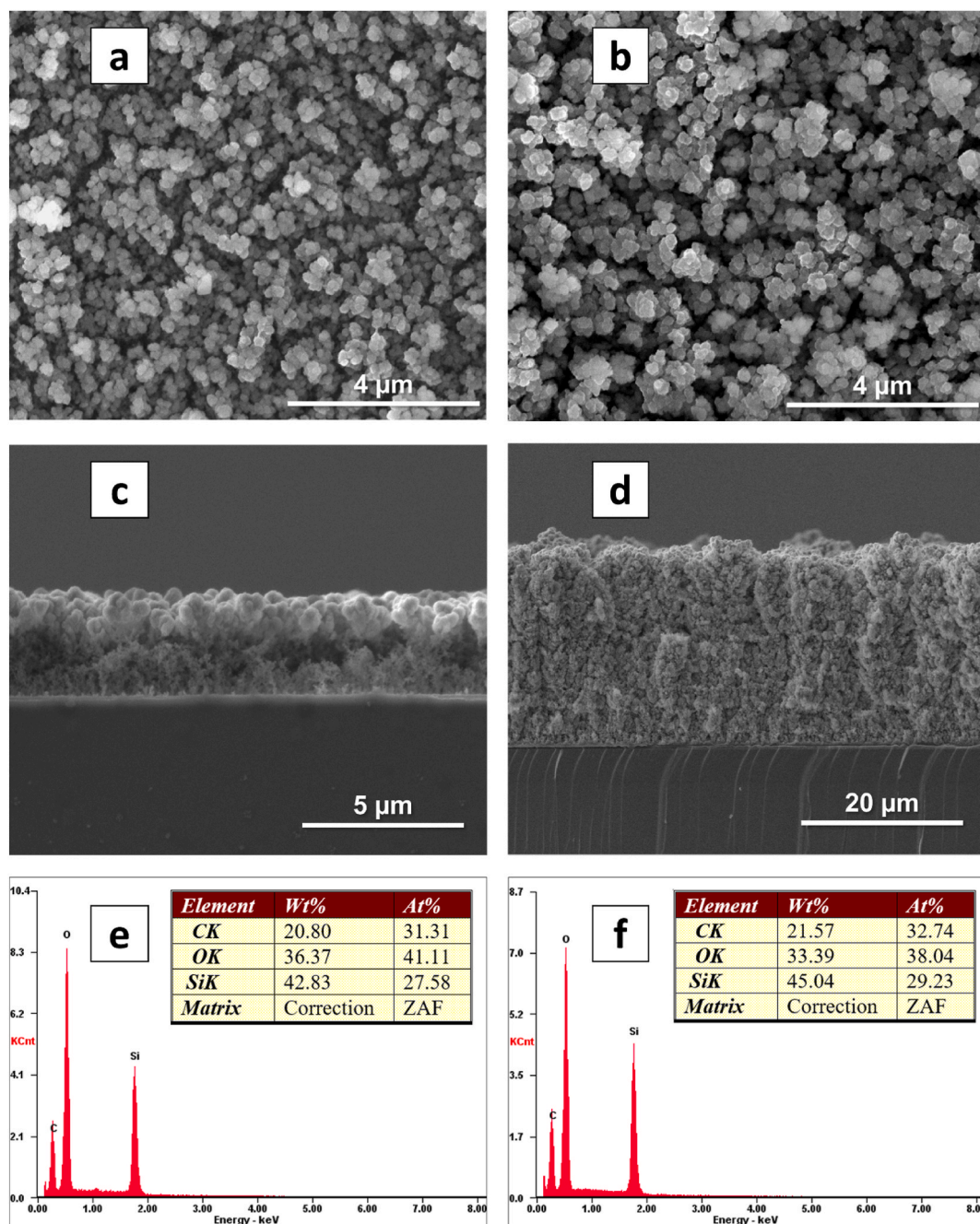


Fig. 4. SEM images of the surface of films deposited on a silicon substrate by plasma polymerisation at atmospheric pressure after one (a) and ten (b) cycles. Cross section of thin films after one (c) and ten (d) cycles. Elemental composition of the films after one (e) and ten (f) cycles. (For interpretation of the references to colour in this figure legend, the reader is referred to the Web version of this article.)

constant at 40 sccm and 1.2 sccm, respectively, and the HMDSO temperature was set at 27 °C (room temperature). The discharge power was varied between 100 W and 200 W in increments of 25 W. Fig. 2a shows the graph of contact angle versus discharge power. It can be seen from the graph that the contact angle increases as the power increases from 140° at 100 W to 165° at 200 W. This indicates that the surface becomes more hydrophobic as the power of the deposition process increases. A larger contact angle indicates that the liquid droplet on the sample surface is more spherical and less able to spread. This behaviour may be due to a change in the morphology and chemical composition of the film with increasing power, affecting its surface properties and interaction with water.

Further studies were carried out to investigate the effect of HMDSO temperature on the contact angle at a constant discharge power (200 W). It should be noted that it can be stated that the HMDSO concentration also varies due to temperature change. The discharge gas flow rate of Ar and HMDSO were set constant: 40 sccm and 1.2 sccm respectively. The HMDSO temperature was varied between 35 °C and 60 °C. From the graph of contact angle versus HMDSO temperature in Fig. 2b, it can be seen that the contact angle almost does not change with increasing HMDSO temperature. This indicates that changing the HMDSO temperature within the considered range has almost no significant effect on the hydrophobicity of the resulting film surface. However, increasing the HMDSO temperature will result in more vapour formation and therefore an increase in the concentration of HMDSO in the injected gas mixture. This can lead to an increase in the rate of film formation and therefore an increase in film thickness. Thus, in this experiment, increasing the HMDSO temperature mainly affects the evaporation process and precursor concentration rather than changing the contact angle and hydrophobicity of the film surface.

The effect of the number of application cycles on the contact angle and transparency of the resulting film was also studied. The discharge gas flow rates of Ar and HMDSO were set constant: 40 sccm and 1.2 sccm respectively, the HMDSO temperature was 27 °C and the discharge power was 200 W. Fig. 3a shows a graph of the contact angle versus the number of cycles. It can be seen from the graph that the contact angle does not change significantly as the number of application cycles increases. The variation of the contact angle is within the measurement error. This means that the number of cycles has no significant effect on the hydrophobicity of the film surface.

The spectra show that the film with 1 deposition cycle has a high transmittance of up to 90 % in the visible spectrum (Fig. 3b).

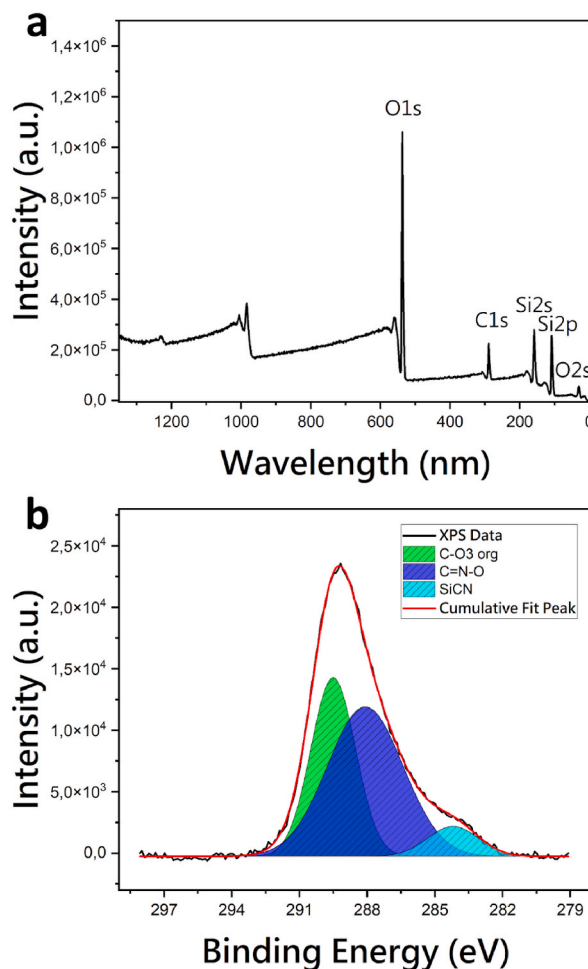


Fig. 5. XPS analysis of the thin film. (a) XPS spectra and (b) deconvoluted C1s peak of the XPS spectra.

However, as the number of deposition cycles increases, the transmittance gradually decreases. This may be due to an increase in film thickness or a change in optical properties with repeated deposition (Fig. 4).

Fig. 4 shows the results of SEM analysis of films deposited on the surface of a silicon substrate by plasma polymerisation at atmospheric pressure with one and ten cycles. From the SEM images of the surface (Fig. 4a and b) it can be seen that the morphology of the films obtained at one and ten cycles is essentially the same. This explains the stability of the superhydrophobic properties and the consistency of the contact angle of the films at different cycles. However, the film thickness measurements show a significant difference between the samples obtained after one and ten cycles. At one deposition cycle, the film thickness is about 3 μm (Fig. 4c), whereas the sample obtained after ten cycles shows a thickness of about 24.5 μm (Fig. 4d). Thus, these results confirm that as the number of deposition cycles increases, the film thickness becomes thicker, which affects its optical transparency. The results of the elemental analysis of the thin films obtained at different cycles are shown in Fig. 4e and f. The analysis shows that the composition of the films does not change with the number of deposition cycles.

Furthermore, XPS analysis was performed to determine the chemical composition and available bonds on the surface of the obtained film. As the results of XPS analysis (Fig. 5a) show, the decomposition products of hexamethyldisiloxane in the plasma environment and the subsequent formation of organosilicon bonds are present on the surface of the samples. The percentages of atomic carbon, oxygen and silicon are given in Table 1. The dominance of oxygen in the spectrum is due to the fact that the experiment is conducted under atmospheric conditions using HMDSO. In addition, it should be noted that the resulting film is porous and has a high degree of roughness, which can lead to large surface oxidation. Fig. 5b shows the XPS spectra of the carbon region (C1s) plotted using the Gaussian approximation. Deconvolution of C1s gave the following peaks: SiCN, C=N-O, C-O3 [44]. SiCN is probably the result of HMDSO decomposition into methyl groups CH₃, Si-O-Si [45], which in turn are fragmented into components and interact with each other to form chemical bonds. The presence of nitrogen bonding in SiCN is attributed to the diffusion of air into the plasma environment. The C=N-O and C-O3 peaks are presumably related to film oxidation or diffusion of oxygen and nitrogen from ambient air into the plasma environment and subsequent deposition on the film with the formation of chemical bonds [46]. The deconvolution of XPS spectra of Si2p and O1s is shown Fig. S3 in the supporting information.

Subsequently, an optical emission spectrum of OES was taken to better understand the film formation mechanism in Ar + HMDSO atmospheric pressure plasma. Fig. 6 shows the results of the optical emission spectrum of Ar plasma (Fig. 6a) and Ar + HMDSO plasma (Fig. 6b). Initially, when pure argon plasma is ignited, intense peaks of atomic argon and some peaks of oxygen and nitrogen are observed. Afterwards, the intensity of argon and oxygen peaks decreases with hexamethyldisiloxane injection. The main explanation is that part of the energy is spent on the dissociation of HMDSO into radicals and on the subsequent chemical reactions of film formation. In the decomposition of HMDSO molecules in RF discharge, the separation of the methyl group CH₃ is the first step of HMDSO fragmentation due to the low bonding energy between Si and CH₃ [46]. The dissociation of methyl groups can be observed by the peaks of SiH and CN which fragmented into H, C and with subsequent chemical reactions with ambient air (O₂, N₂) [47]. The presence of SiO emission lines and Si atomic spectrum (4s->3p, 3p->3s) [48] indicates the fragmentation of the Si-O-Si bond. The identified nitrogen-containing components in the plasma and in the film are due to the diffusion of ambient air into the active region of the plasma flow.

The films obtained were tested for stability and durability of hydrophobic properties under extreme conditions, in particular the effects of UV irradiation, high temperatures, chemical reagents and durability under weathering conditions. The concentration (temperature) of HMDSO and the number of cycles did not affect the superhydrophobic properties. For further studies, superhydrophobic surface experiments were carried out at room temperature and 1 cycle.

The chemical test was carried out using three different chemicals: ethanol, acetone and 646 solvent. The chemical test procedure was as follows: three samples were taken and the contact angle of each was measured before the test. Each sample was then placed on a flask containing the appropriate chemical for 1 h. The film was then left outdoors for 24 h to allow the chemicals to evaporate completely and the contact angle was measured after the test. Fig. 7a shows that the hydrophobic properties of the films obtained remained almost unchanged after the chemical test. This indicates that chemical reagents such as ethanol, acetone and 646 solvent do not have a destructive effect on the superhydrophobic films. It can therefore be concluded that these films are resistant to chemical influences.

UV resistance was tested using a 100 W UV lamp with a wavelength of 250 nm. The film was exposed to UV irradiation for 1 h at 10-min intervals and the contact angle is measured before and after each irradiation step. The change in contact angle before and after irradiation is shown in Fig. 7b. As can be seen from the graph, UV irradiation has no visible effect on the hydrophobic properties of the films obtained. The contact angle is largely unchanged after irradiation, indicating that the films are resistant to UV irradiation. This indicates that the films have good UV resistance and retain their hydrophobic properties even with prolonged irradiation.

The thermal test was carried out using a heater. After reaching a certain temperature, we left the film on the heater for 30 min. The contact angle was measured before and after the test. The dependence of the contact angle on temperature is shown in Fig. 7c. It can be seen from the graph that high temperatures, even up to 400°, have almost no effect on the hydrophobic properties of the obtained film.

Table 1
Quantitative analysis of the chemical composition of the surface.

	Start BE	Peak BE	End BE	FWHM eV	Atomic %
O1s	542.58	537.09	523.08	4.18	58.14
Si2p	110.08	107.4	94.08	4.13	21.88
C1s	296.08	289.16	281.58	4.03	19.98

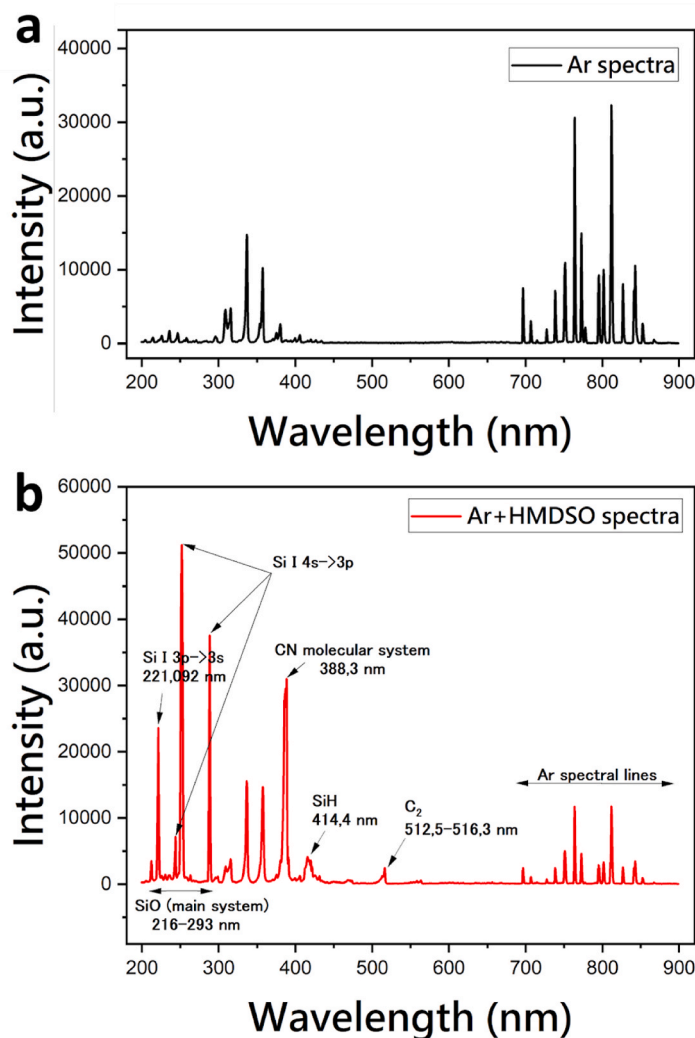


Fig. 6. Optical emission spectrum of Ar plasma (a) and Ar + HMDSO plasma (b).

An insignificant decrease of the contact angle is observed which is within the measurement error of the goniometer. This indicates high thermal stability and preservation of the hydrophobic properties of the film at critical temperatures.

The obtained superhydrophobic films were subjected to a 16-month durability test in Almaty weather conditions. The average temperature in the region ranges from $-11\text{ }^{\circ}\text{C}$ in winter to $30\text{ }^{\circ}\text{C}$ in summer, rarely dropping below $-18\text{ }^{\circ}\text{C}$ or rising above $34\text{ }^{\circ}\text{C}$ [49]. The contact angle was measured before the start of the experiment and monthly thereafter. The sample was exposed to a variety of weather conditions, including heavy rain, snow, frost, direct sunlight and heat. Fig. 7d shows a graph of the contact angle versus time of exposure to weather conditions. The graph shows that the obtained superhydrophobic films show their stability in extreme weather conditions. The contact angle is virtually unchanged throughout the test period, indicating that the films retain their hydrophobic properties. This indicates that the films are highly resistant and are able to retain their functionality even when exposed to prolonged exposure to aggressive weather conditions. Thus, the results of the study confirm that the superhydrophobic films obtained by atmospheric plasma polymerisation are weather resistant and can be successfully applied in real climatic conditions, including extreme temperatures and exposure to solar radiation.

Finally, the self-cleaning property of the resulting superhydrophobic films was investigated. The self-cleaning property of the surface plays an important role in practical applications such as solar panels and architectural glass exterior walls, as it allows the automatic removal of contaminants without additional energy input. As shown in Fig. 8b, when a drop of water rolls over the superhydrophobic coating, contaminants on the surface are easily removed by the water drop, leaving the surface clean. Moreover, as the number of drips increases, the water removes more and more contaminants, indicating the superior self-cleaning characteristics of the superhydrophobic coating. In contrast, when the same test is performed on clean glass (Fig. 8a), traces of water droplets remain on the surface and contamination is not removed, indicating the inadequate self-cleaning ability of clean glass. The difference in the self-cleaning characteristics of superhydrophobic film and clear glass can be explained by their different adhesion properties to water. The

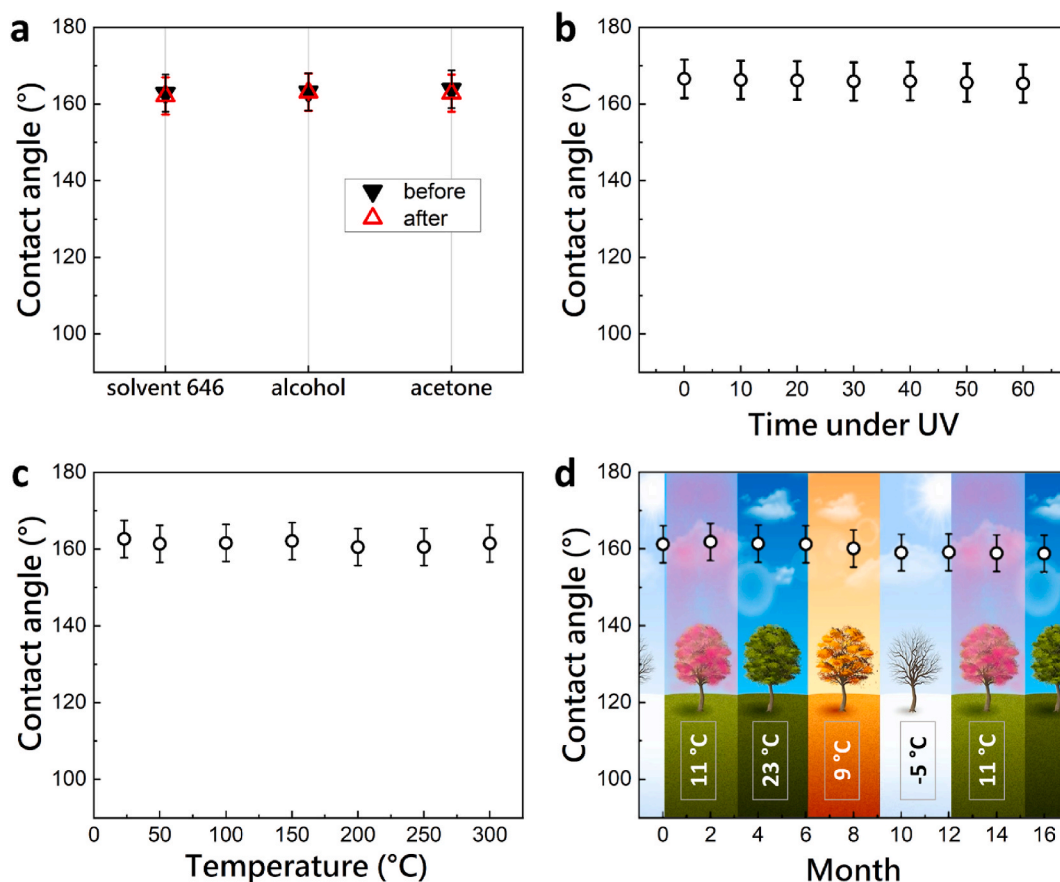


Fig. 7. Contact angle graphs of obtained films from chemical tests (a), UV tests (b), thermal tests (c), time (d).

surface of clear glass contains a large number of hydrophilic hydroxyl groups, which gives the surface a strong affinity to water. As a result, a drop of water remains on the surface of pure glass. In turn, films formed by HMDSO plasma polymerisation at atmospheric pressure are superhydrophobic and have very low adhesion to water. Water droplets can therefore easily roll off the superhydrophobic coating, taking the dirt with them (a video of testing the self-cleaning properties of the coating is shown in [video S2](#) in the accompanying information). These results show that the superhydrophobic coating obtained in this work can be used as a self-cleaning surface. This opens up the prospect of applications in various areas where maintaining a clean surface is important, such as solar panels and architectural glass.

In order to investigate the capability of plasma technology at atmospheric pressure in a variety of applications, we have applied hydrophobic coatings on a variety of materials including polyvinyl chloride (PVC) (Fig. 9a), plastic (Fig. 9b), glass (Fig. 9c), corundum (Fig. 9d), fabric (Fig. 9e) and paper (Fig. 9f). The figures show that the treated samples have the ability to repel water, providing long-term protection against moisture. Water droplets on these surfaces roll off easily without leaving traces or penetrating the material. The resulting hydrophobic coatings have a wide range of applications in various fields such as construction, industry, textile production and many others where reliable protection of materials against moisture and water is crucial. Thus, this technology can be successfully applied in various practical fields.

4. Conclusion

In this work, superhydrophobic films were successfully produced using HMDSO plasma polymerisation method in an RF discharge plasma jet at atmospheric pressure. 3D printing technology was used to apply the films, allowing the superhydrophobic coating to be applied on a large scale. The study showed that the contact angle of the films was directly related to the RF discharge power. HMDSO concentration and number of cycles have no effect on the superhydrophobic properties of the film but do affect the optical properties, resulting in reduced light transmission. Under optimal conditions, a contact angle of about 165° is achieved, providing a highly hydrophobic surface. When the film was applied in a single layer, the transmittance at 700 nm was about 88 %, compared to 92 % for pure glass. Surface morphological and chemical characterisation was carried out using SEM, demonstrating that the plasma jet is able to create micro- and nanostructured coatings with high surface roughness, giving the surface a superhydrophobic property. The resulting superhydrophobic films also demonstrated stability and resistance to chemical solutions, high temperatures, UV irradiation

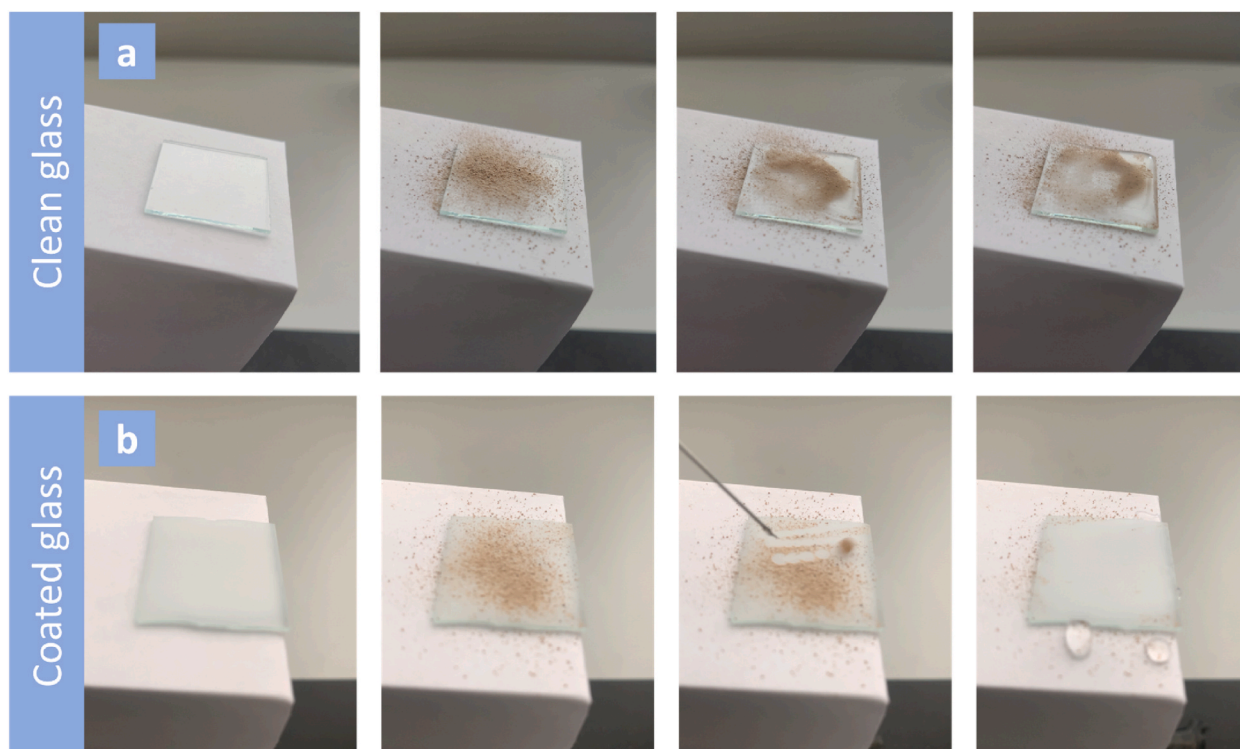


Fig. 8. Self-cleaning property test without deposition (a) and with deposition (b).

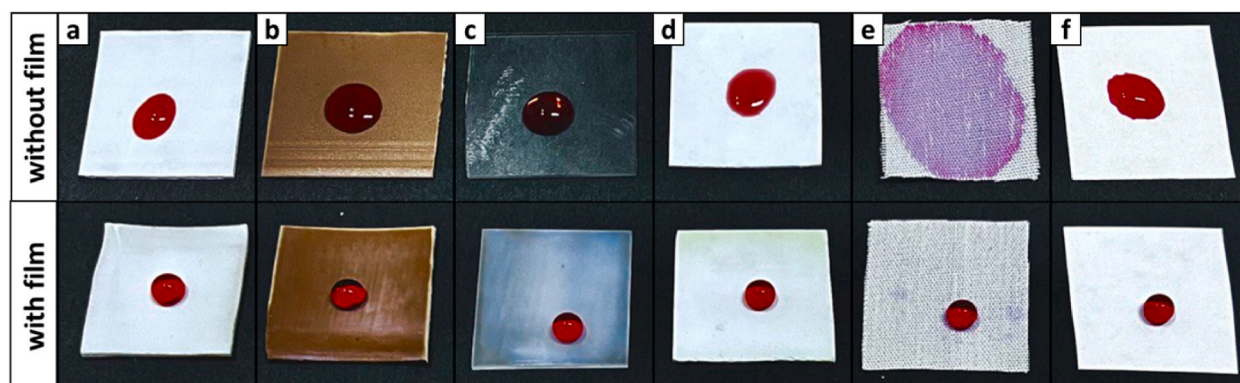


Fig. 9. Obtaining a hydrophobic coating on different materials: PVC (a), plastic (b), glass (c), corundum (d), fabric (e), paper (f).

and the weather. This method of producing stable and durable superhydrophobic films by HMDSO plasma polymerisation at atmospheric pressure can be applied to a variety of applications including automotive, construction, electronics, medical and others where protection of the surface against moisture, dirt and corrosion is required.

CRedit authorship contribution statement

Sultan Ussenkhan: Writing – original draft, Visualization, Investigation, Formal analysis. Baglan Kyrykbay: Investigation. Yerlanuly Yerassyl: Writing – review & editing, Writing – original draft, Supervision, Methodology, Data curation, Conceptualization. Askar Zhunisbekov: Resources, Methodology. Maratbek Gabdullin: Resources, Methodology. Tlekkabul Ramazanov: Resources, Methodology. Sagi Orazbayev: Supervision, Project administration, Funding acquisition. Almasbek U. Utegenov: Writing – review & editing, Methodology

Financial disclosure

This research was funded by the Committee of Science of the Ministry of Science and Higher Education of the Republic of Kazakhstan (Grant No. AP13067865).

Data availability statement

The data that support the findings of this study are available from the corresponding author upon reasonable request.

Declaration of competing interest

The authors declare that they have no known competing financial interests or personal relationships that could have appeared to influence the work reported in this paper.

Acknowledgments

All authors are grateful for the Committee of Science of the Ministry of Science and Higher Education of the Republic of Kazakhstan (Grant No. AP13067865).

Appendix A. Supplementary data

Supplementary data to this article can be found online at <https://doi.org/10.1016/j.heliyon.2023.e23844>.

References

- [1] Y. Wang, H. Zhang, X. Liu, Z. Zhou, Slippery liquid-infused substrates: a versatile preparation, unique anti-wetting and drag-reduction effect on water, *J. Mater. Chem. A* 4 (2016) 2524–2529, <https://doi.org/10.1039/C5TA09936F>.
- [2] Y.-Y. Ji, S.-S. Kim, O.-P. Kwon, S.-H. Lee, Easy fabrication of large-size superhydrophobic surfaces by atmospheric pressure plasma polymerization with non-polar aromatic hydrocarbon in an in-line process, *Appl. Surf. Sci.* 255 (2009) 4575–4578, <https://doi.org/10.1016/j.apsusc.2008.12.002>.
- [3] Y. Si, Z. Dong, L. Jiang, Bioinspired designs of superhydrophobic and superhydrophilic materials, *ACS Cent. Sci.* 4 (2018) 1102–1112, <https://doi.org/10.1021/acscentsci.8b00504>.
- [4] J.H. Yim, V. Rodriguez-Santiago, A.A. Williams, T. Gougousi, D.D. Pappas, J.K. Hirvonen, Atmospheric pressure plasma enhanced chemical vapor deposition of hydrophobic coatings using fluorine-based liquid precursors, *Surf. Coating. Technol.* 234 (2013) 21–32, <https://doi.org/10.1016/j.surfcoat.2013.03.028>.
- [5] C. Qi, H. Chen, Y. Sun, Q. Fu, L. Shen, X. Li, Y. Liu, Facile synthesis and anti-icing performance of superhydrophobic flower-like OTS-SiO₂ with tunable size, *Adv. Powder Technol.* 31 (2020) 4533–4540, <https://doi.org/10.1016/j.apt.2020.09.029>.
- [6] Z. Li, Z. Guo, Bioinspired surfaces with wettability for antifouling application, *Nanoscale* 11 (2019) 22636–22663, <https://doi.org/10.1039/C9NR05870B>.
- [7] K.B. Golovin, J.W. Gose, M. Perlin, S.L. Ceccio, A. Tuteja, Bioinspired surfaces for turbulent drag reduction, *Phil. Trans. Math. Phys. Eng. Sci.* 374 (2016), 20160189, <https://doi.org/10.1098/rsta.2016.0189>.
- [8] S. Brown, J. Lengaigne, N. Sharifi, M. Pugh, C. Moreau, A. Dolatabadi, L. Martinu, J.E. Klemberg-Sapieha, Durability of superhydrophobic duplex coating systems for aerospace applications, *Surf. Coating. Technol.* 401 (2020), 126249, <https://doi.org/10.1016/j.surfcoat.2020.126249>.
- [9] K. Gotoh, E. Shohbuke, G. Ryu, Application of atmospheric pressure plasma polymerization for soil guard finishing of textiles, *Textil. Res. J.* 88 (2018) 1278–1289, <https://doi.org/10.1177/0040517517698988>.
- [10] P. Sundriyal, S. Bhattacharya, Polyaniline silver nanoparticle coffee waste extracted porous graphene oxide nanocomposite structures as novel electrode material for rechargeable batteries, *Mater. Res. Express* 4 (2017), 035501, <https://doi.org/10.1088/2053-1591/aa5e3e>.
- [11] J. Wu, J. He, K. Yin, Z. Zhu, S. Xiao, Z. Wu, J.-A. Duan, Robust hierarchical porous PTFE film fabricated via femtosecond laser for self-cleaning passive cooling, *Nano Lett.* 21 (2021) 4209–4216, <https://doi.org/10.1021/acs.nanolett.1c00038>.
- [12] Y. Zhu, F. Yang, Z. Guo, Bioinspired surfaces with special micro-structures and wettability for drag reduction: which surface design will be a better choice? *Nanoscale* 13 (2021) 3463–3482, <https://doi.org/10.1039/D0NR07664C>.
- [13] Q. Chao, L. Meng, C. Shuxian, Anti-icing characteristics of PTFE super hydrophobic coating on titanium alloy surface, *J. Alloys Compd.* 860 (2021), 157907, <https://doi.org/10.1016/j.jallcom.2020.157907>.
- [14] C. Lv, H. Wang, Z. Liu, W. Zhang, C. Wang, R. Tao, M. Li, Y. Zhu, A sturdy self-cleaning and anti-corrosion superhydrophobic coating assembled by amino silicon oil modifying potassium titanate whisker-silica particles, *Appl. Surf. Sci.* 435 (2018) 903–913, <https://doi.org/10.1016/j.apsusc.2017.11.205>.
- [15] T. Zhu, S. Li, J. Huang, M. Mihailiasa, Y. Lai, Rational design of multi-layered superhydrophobic coating on cotton fabrics for UV shielding, self-cleaning and oil-water separation, *Mater. Des.* 134 (2017) 342–351, <https://doi.org/10.1016/j.matdes.2017.08.071>.
- [16] Y.S. You, S. Kang, R. Mauchauffé, S.Y. Moon, Rapid and selective surface functionalization of the membrane for high efficiency oil-water separation via an atmospheric pressure plasma process, *Sci. Rep.* 7 (2017), 15345, <https://doi.org/10.1038/s41598-017-15713-x>.
- [17] S. Pan, R. Guo, M. Björnalm, J.J. Richardson, L. Li, C. Peng, N. Bertleff-Zieschang, W. Xu, J. Jiang, F. Caruso, Coatings super-repellent to ultralow surface tension liquids, *Nat. Mater.* 17 (2018) 1040–1047, <https://doi.org/10.1038/s41563-018-0178-2>.
- [18] J. Zhang, S. Seeger, Superoleophobic coatings with ultralow sliding angles based on silicone nanofilaments, *Angew. Chem. Int. Ed.* 50 (2011) 6652–6656, <https://doi.org/10.1002/anie.201101008>.
- [19] E. Celia, T. Darmanin, E. Taffin de Givenchy, S. Amigoni, F. Guittard, Recent advances in designing superhydrophobic surfaces, *J. Colloid Interface Sci.* 402 (2013) 1–18, <https://doi.org/10.1016/j.jcis.2013.03.041>.
- [20] A.K. Gnanappa, E. Gogolides, F. Evangelista, M. Riepen, Contact line dynamics of a superhydrophobic surface: application for immersion lithography, *Microfluid. Nanofluidics* 10 (2011) 1351–1357, <https://doi.org/10.1007/s10404-010-0762-5>.
- [21] D.M. Spori, T. Drobek, S. Zürcher, N.D. Spencer, Cassie-state wetting investigated by means of a hole-to-pillar density gradient, *Langmuir* 26 (2010) 9465–9473, <https://doi.org/10.1021/la904714c>.
- [22] M.A.S. Chong, Y.B. Zheng, H. Gao, L.K. Tan, Combinational template-assisted fabrication of hierarchically ordered nanowire arrays on substrates for device applications, *Appl. Phys. Lett.* 89 (2006), <https://doi.org/10.1063/1.2399935>.

- [23] Y. Zhao, Z. Xu, X. Wang, T. Lin, Photoreactive azido-containing silica nanoparticle/polycation multilayers: durable superhydrophobic coating on cotton fabrics, *Langmuir* 28 (2012) 6328–6335, <https://doi.org/10.1021/la300281q>.
- [24] T. Wang, T.T. Isimjan, J. Chen, S. Rohani, Transparent nanostructured coatings with UV-shielding and superhydrophobicity properties, *Nanotechnology* 22 (2011), 265708, <https://doi.org/10.1088/0957-4484/22/26/265708>.
- [25] J. Shao, K. Fu, Y. Liu, S. Xu, Z. Sun, M. Cao, Y. Liu, X. Wang, Y. Zhou, Fluorine-functionalized mesoporous alumina materials with superhydrophobic surfaces, *Surface. Interfac.* 40 (2023), 103046, <https://doi.org/10.1016/j.surf.2023.103046>.
- [26] A. Tombesi, S. Li, S. Sathasivam, K. Page, F.L. Heale, C. Pettinari, C.J. Carmalt, I.P. Parkin, Aerosol-assisted chemical vapour deposition of transparent superhydrophobic film by using mixed functional alkoxysilanes, *Sci. Rep.* 9 (2019) 7549, <https://doi.org/10.1038/s41598-019-43386-1>.
- [27] M. Liu, X. Tan, X. Li, J. Geng, M. Han, K. Wei, X. Chen, Transparent superhydrophobic EVA/SiO₂/PTFE/KH-570 coating with good mechanical robustness, chemical stability, self-cleaning effect and anti-icing property fabricated by facile dipping method, *Colloids Surf. A Physicochem. Eng. Asp.* 658 (2023), 130624, <https://doi.org/10.1016/j.colsurfa.2022.130624>.
- [28] Y. Li, C. Zou, J. Shao, X. Zhang, Y. Li, Preparation of SiO₂/PS superhydrophobic fibers with bionic controllable micro–nano structure via centrifugal spinning, *RSC Adv.* 7 (2017) 11041–11048, <https://doi.org/10.1039/C6RA25813A>.
- [29] S. Orazbayev, R. Zhumadilov, A. Zhunisbekov, M. Gabdullin, Y. Yerlanuly, A. Utegenov, T. Ramazanov, Superhydrophobic carbonous surfaces production by PECVD methods, *Appl. Surf. Sci.* 515 (2020), 146050, <https://doi.org/10.1016/j.apsusc.2020.146050>.
- [30] C.-W. Kan, C.-H. Kwong, S.-P. Ng, Atmospheric pressure plasma surface treatment of rayon flock synthetic leather with tetramethylsilane, *Appl. Sci.* 6 (2016) 59, <https://doi.org/10.3390/app6020059>.
- [31] G. Mertz, M. Delmée, J. Bardon, A. Martin, D. Ruch, T. Fouquet, S. Garreau, A. Airoudj, A. Marguier, L. Ploux, V. Roucoules, Atmospheric pressure plasma copolymerization of two acrylate precursors: toward the control of wetting properties, *Plasma Process. Polym.* 15 (2018), <https://doi.org/10.1002/ppap.201800073>.
- [32] S. Orazbayev, M. Gabdullin, T. Ramazanov, M. Dosbolayev, D. Omirbekov, Y. Yerlanuly, Obtaining of superhydrophobic surface in RF capacitively coupled discharge in AR/CH₄ medium, *Appl. Surf. Sci.* 472 (2019) 127–134, <https://doi.org/10.1016/j.apsusc.2018.03.118>.
- [33] R. Jafari, S. Asadollahi, M. Farzaneh, Applications of plasma technology in development of superhydrophobic surfaces, *Plasma Chem. Plasma Process.* 33 (2013) 177–200, <https://doi.org/10.1007/s11090-012-9413-9>.
- [34] J.A.S. Ting, L.M.D. Rosario, H.V. Lee, H.J. Ramos, R.B. Tumlos, Hydrophobic coating on glass surfaces via application of silicone oil and activated using a microwave atmospheric plasma jet, *Surf. Coating. Technol.* 259 (2014) 7–11, <https://doi.org/10.1016/j.surfcoat.2014.08.008>.
- [35] B. Balu, V. Breedveld, D.W. Hess, Fabrication of “roll-off” and “sticky” superhydrophobic cellulose surfaces via plasma processing, *Langmuir* 24 (2008) 4785–4790, <https://doi.org/10.1021/la703766c>.
- [36] X.J. Feng, L. Jiang, Design and creation of superwetting/antiwetting surfaces, *Adv. Mater.* 18 (2006) 3063–3078, <https://doi.org/10.1002/adma.200501961>.
- [37] D. Ebert, B. Bhushan, Transparent, superhydrophobic, and wear-resistant coatings on glass and polymer substrates using SiO₂, ZnO, and ITO nanoparticles, *Langmuir* 28 (2012) 11391–11399, <https://doi.org/10.1021/la301479c>.
- [38] J.A. Howarter, J.P. Youngblood, Self-cleaning and next generation anti-fog surfaces and coatings, *Macromol. Rapid Commun.* 29 (2008) 455–466, <https://doi.org/10.1002/marc.200700733>.
- [39] E. Yu, S.-C. Kim, H.J. Lee, K.H. Oh, M.-W. Moon, Extreme wettability of nanostructured glass fabricated by non-lithographic, anisotropic etching, *Sci. Rep.* 5 (2015) 9362, <https://doi.org/10.1038/srep09362>.
- [40] F. Liu, M. Cai, B. Zhang, Z. Fang, C. Jiang, K. (Ken, Ostrikov, Hydrophobic surface modification of polymethyl methacrylate by two-dimensional plasma jet array at atmospheric pressure, *J. Vac. Sci. Technol. A: Vacuum, Surfaces, and Films* (2018) 36, <https://doi.org/10.1116/1.5030718>.
- [41] K. Aumaille, C. Vallée, A. Granier, A. Goulet, F. Gaboriau, G. Turban, A comparative study of oxygen/organosilicon plasmas and thin SiOx/CyHz films deposited in a helicon reactor, *Thin Solid Films* 359 (2000) 188–196, [https://doi.org/10.1016/S0040-6090\(99\)00883-4](https://doi.org/10.1016/S0040-6090(99)00883-4).
- [42] D.S. Wavhal, J. Zhang, M.L. Steen, E.R. Fisher, Investigation of gas phase species and deposition of SiO₂ films from HMDSO/O₂ plasmas, *Plasma Process. Polym.* 3 (2006) 276–287, <https://doi.org/10.1002/ppap.200500140>.
- [43] C. Chaiwong, P. Rachtanapun, S. Sarapirom, D. Boonyawan, Plasma polymerization of hexamethyldisiloxane: Investigation of the effect of carrier gas related to the film properties, *Surf. Coating. Technol.* 229 (2013) 12–17, <https://doi.org/10.1016/j.surfcoat.2012.08.058>.
- [44] The international XPS database of XPS spectra, (n.d.). <https://xpsdatabase.net> (accessed November 17, 2023)..
- [45] M. Quitzau, M. Wolter, V. Zaporozhtchenko, H. Kersten, F. Faupel, Modification of polyethylene powder with an organic precursor in a spiral conveyor by hollow cathode glow discharge, *The European Physical Journal D* 58 (2010) 305–310, <https://doi.org/10.1140/epjd/e2010-00121-9>.
- [46] J. Li, Q. Yuan, X. Chang, Y. Wang, G. Yin, C. Dong, Deposition of organosilicone thin film from hexamethyldisiloxane (HMDSO) with 50 kHz/33 MHz dual-frequency atmospheric-pressure plasma jet, *Plasma Sci. Technol.* 19 (2017), 045505, <https://doi.org/10.1088/2058-6272/aa57e4>.
- [47] A. Kilicaslan, O. Levasseur, V. Roy-Garofano, J. Profili, M. Moisan, C. Côté, A. Sarkissian, L. Stafford, Optical emission spectroscopy of microwave-plasmas at atmospheric pressure applied to the growth of organosilicon and organotitanium nanopowders, *J. Appl. Phys.* 115 (2014), <https://doi.org/10.1063/1.4868899>.
- [48] Atomic spectra database, (n.d.). <https://www.nist.gov/pml/atomic-spectra-database> (accessed November 17, 2023).
- [49] <https://weatherspark.com/y/108859/Average-Weather-in-Almaty-Kazakhstan-Year-Round.>, ((n.d.)).